

Thermal-mechanical Coupling Analysis of Split Mechanical Seals

Jingde Wang, Guanglei Zeng, Heshun Wang*, Weibing Zhu

University of Mechanical Engineering, Xihua University, Chengdu, Sichuan 610039, China

*Corresponding author: Heshun Wang (Email: wangheshun@mail.xhu.edu.cn)

Abstract

In order to study the effects of frictional heat and medium pressure on the deformation of split mechanical seals, thermal-mechanical coupling numerical analysis of split mechanical seals was carried out. The results show that: in the temperature field, the temperature on the outer diameter side of the seal ring is lower, the highest temperature of the end face of the split dynamic ring appears at the seal end face that is in contact with the split static ring, and the highest temperature of the end face of the split static ring appears at the inner diameter of the seal end face; Under the action of heat and force coupling, the sealing end face forms a convergent gap from the deformation of the outer diameter to the inner diameter; as the medium pressure increases, the axial deformation of the sealing ring increases, and the radial deformation of the sealing ring parting surface decreases; The change of medium pressure leads to the difference of frictional heat generated between the end faces of the sealing ring, which causes the difference of the deformation of the sealing ring.

Keywords

Split Mechanical Seal; Thermomechanical Coupling; Parting Surface.

1. Introduction

In industrial fields such as petrochemical engineering, electric power energy, and water treatment, the rotary shaft seal serves as a key component, whose sealing performance is directly related to the safety, economy, and environmental protection of production. Although the conventional integrated mechanical seal features high sealing reliability, it requires equipment disassembly during maintenance and overhaul, which is time-consuming and labor-intensive, resulting in long shutdown periods and seriously affecting the efficiency of continuous industrial production. Compared with traditional mechanical seals, split mechanical seals are convenient for installation and disassembly, economically efficient, and avoid major disassembly during replacement^[1]. Against this background, split mechanical seals have gradually become an important direction for sealing upgrading of large-scale rotating equipment.

A split mechanical seal is formed by cutting a complete ring into two halves, and the split ring and its holder are connected by screws and pins or clamped by a clamping ring^[3]. However, the introduction of the split structure also brings new technical challenges: the existence of the split surface breaks the structural integrity of the seal ring, leading to uneven stiffness distribution. Under the action of working pressure, temperature, centrifugal force and other loads, asymmetric deformation is prone to occur, which further causes problems such as poor fitting of the sealing end face and abnormal clearance, possibly reducing sealing performance and even leading to seal failure^[4]. Therefore, an in-depth study on the deformation law and influencing factors of split mechanical seals is the key to improving their sealing reliability and engineering application value.

2. Sealing Structure and Working Condition Parameters

2.1 Structural Parameters and Working Condition Parameters

In this paper, two kinds of split mechanical seal models are analyzed. The core difference is the circumferential position of the static ring and the static ring seat: the split surfaces of Scheme 1 are coplanar, and the split surfaces of Scheme 2 (designed in this paper) are staggered 90 circumferentially. The model is constructed and simplified by UG software, which is composed of split moving ring, static ring and static ring seat. The geometric structure is shown in Fig. 1, and the structural parameters are shown in Table 1.

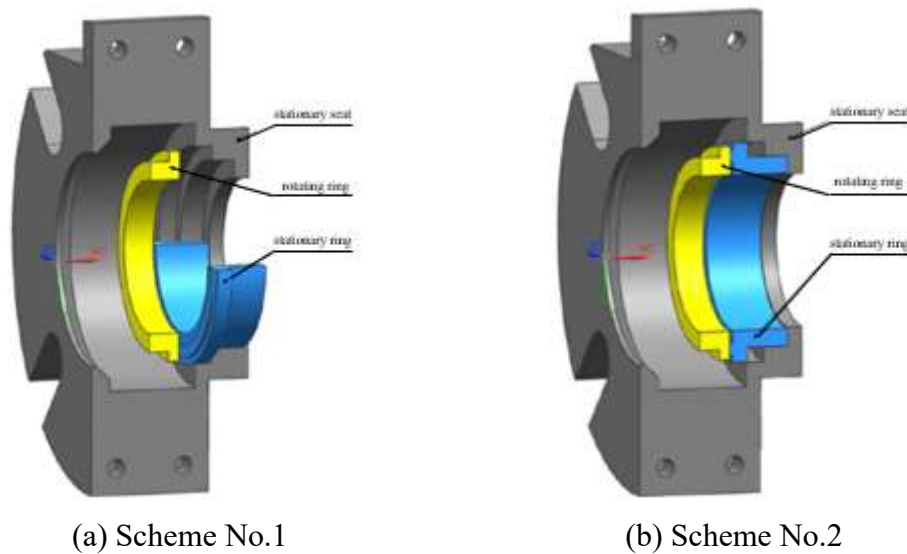


Fig. 1 model schematic diagram

Table 1. Main Structure Size Range

Parameter	WIHS
Back thickness l of Rotating ring (l /mm)	2~4
Thickness of the stationary ring back (l_2 /mm)	3.2~5.2
Back height of rotating ring (h_2 /mm)	1.85~3.85
Back height of stationary ring (h_1 /mm)	2.2~4.2
Thickness of stationary ring boss (l_1 /mm)	2
Face width of stationary ring (b /mm)	3

2.2 Calculation of Boundary Conditions

2.2.1 Working Conditions Parameters

According to the actual working conditions of the seal, the spindle speed is set to 1500 r/min, the spring specific pressure is 0.15 MPa, and the medium is clean water at 50 °C with a pressure of 0.5 MPa. The materials of the rotating ring and stationary ring are both selected as SiC, and their main performance parameters are listed as follows: Density:3200 kg/m³;Elastic Modulus: 380 GPa;Poisson's ratio:0.3;Thermal conductivity: 100 W/(m·K); Thermal expansion coefficient (K⁻¹).

2.2.2 Thermal calculation

Under normal operating conditions of a dry gas seal, the main heat source is the gas viscous friction heat generated by the seal end face. The calculation formula of viscous friction heat is^[7]:

$$Q = fF_c v \tag{1}$$

$$v = \frac{2\pi rn}{60} \tag{2}$$

In the formula, f is the heat friction coefficient; F_c is the face pressure, Pa; r is the outer radius of the seal ring, m. n is the rotational speed, r/min. There are various methods for calculating frictional heat distribution, some scholars have obtained relevant conclusions through experiments or numerical verification. In this paper, the end-face heat distribution is calculated using the corresponding formula^[8].

$$\frac{q_s}{q} = \frac{1}{1 + \frac{h_s \lambda_w}{h_w \lambda_s}} \tag{3}$$

In the formula, q_w is the heat flux of the rotating ring, W/m²; q_s is the heat flux of the stationary ring; λ_s is the thermal conductivity of the stationary ring, W/(m·K); h is the axial thickness of the seal ring, m. For the convective boundary, the following formula is used for calculation^[10]:

$$\alpha = \frac{k}{D} \times 0.135 [(0.5R_{ec}^2 + R_{rf}^2) p_r]^{0.33} \tag{4}$$

In the formula, α is the convective heat transfer coefficient, W/(m²·K); D is the outer diameter of the seal ring, m; R_{ec} is the rotational stirring effect of the medium. R_{rf} is the transverse flow effect of the medium. v_z is the axial flow velocity of the medium, m/s. ν is the kinematic viscosity of the fluid, m²/s. All other boundaries are regarded as adiabatic boundaries, and the convective heat transfer coefficient is 0

3. Thermo-structural Coupling Analysis of Split Mechanical Seal

3.1 Result Analysis of Temperature Field in Seal Ring

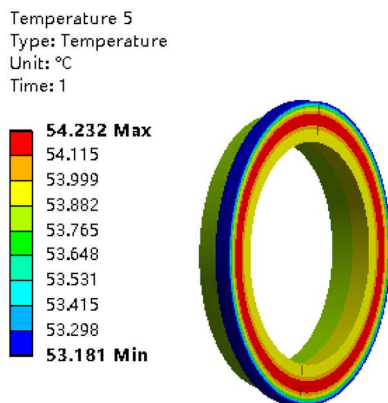


Fig. 2 Temperature of the rotating ring

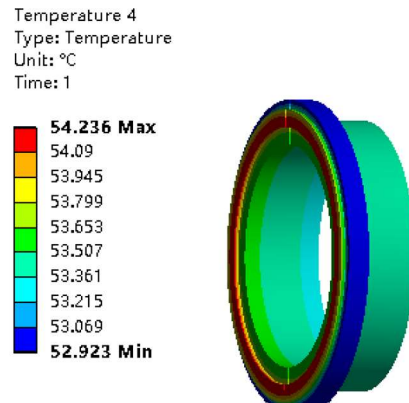


Fig. 3 Temperature of the stationary ring

Taking Scheme 2 as the research object, under the working conditions of spindle speed 1500 r/min, spring specific pressure 0.15 MPa, and medium pressure at the corresponding set value, the calculated

temperature field results of the seal ring are shown in Fig. 2 and Fig. 3. The analysis shows that there is a certain temperature difference between the rotating ring and the stationary ring, in which the extreme temperature of the stationary ring is slightly higher than that of the rotating ring, and both show the same temperature distribution trend: In the axial direction, the temperature decreases gradually from the sealing end face outward; in the radial direction, the temperature decreases from the sealing end face toward both the inner and outer diameters.

3.2 Thermo-structural Coupling Boundary Conditions Setting

The temperature field results are imported into the static analysis, and the static boundary conditions are added. The mechanical boundary conditions are shown in Table 2.

Table 2. Mechanical Boundary Conditions of the Seal Ring

Mechanical Boundary Conditions	Boundary
Medium Pressure / MPa	5-6,6-7,7-8,8-9,9-10,10-11,11-12
Spring Specific Pressure / MPa	3-4
Liquid Film Pressure / MPa	1-8

3.3 Deformation Law of the Seal Ring

Under the combined action of thermal and mechanical loads, the seal ring undergoes deformation, as shown in Fig. 4. The deformation mainly occurs at the sealing end face and the split surfaces. It can be seen that the sealing end face is convergent and opens outward, and gaps appear at the split surfaces of both the split stationary ring and the split rotating ring.

This is caused by the uneven heat distribution generated by friction, which results in different deformation amounts between the inner diameter side and the outer diameter side of the seal ring.

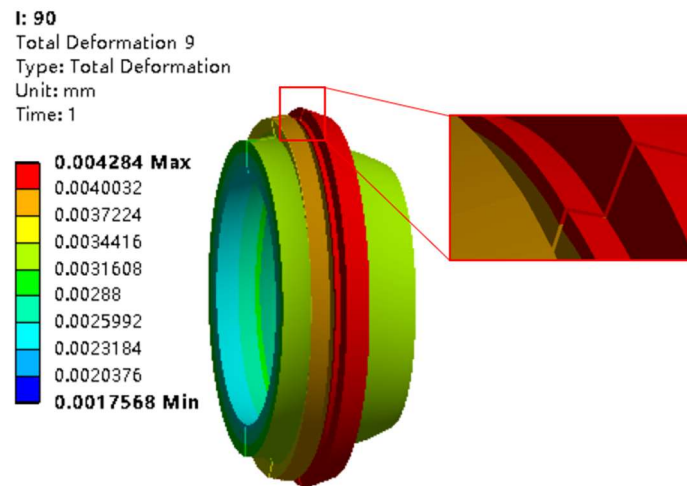


Fig. 4 Total Deformation Contour of the Seal Ring

According to the deformation of the seal ring, gaps are formed at both the sealing end face and the split surface, which can be studied specifically.

It can be seen from Fig. 5 that the axial deformation of the rotating ring and the stationary ring at the inner diameter is consistent, while the axial deformation at the outer diameter is different and the deformation directions are opposite. The two rings are closely fitted at the inner diameter. As the radius increases to a certain position, the end faces of the two rings gradually separate, forming a convergent gap.

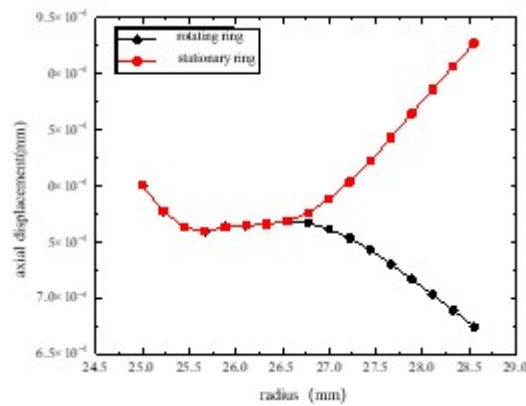


Fig. 5 Axial Deformation Curve vs. Radius

It can be seen from Fig. 6 that under the same working conditions, the circumferential deformation of the stationary ring is larger than that of the rotating ring, that is, the convergent gap opening at the split surface of the stationary ring is larger.

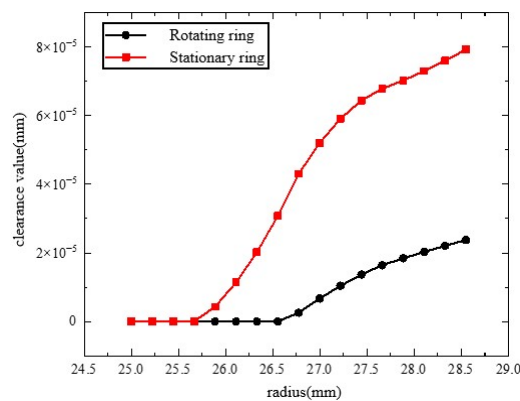


Fig. 6 Circumferential Gap Curve vs. Radius

3.4 Influence of Structural Parameters on Deformation and Stress of Seal Ring

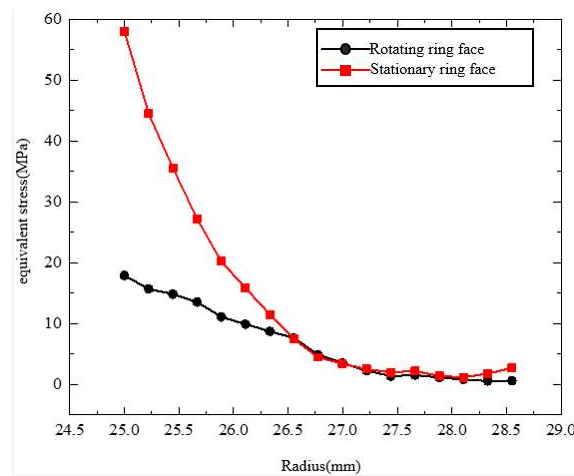


Fig. 7 Equivalent Stress Curve of Seal Ring End Face vs. Radius

The equivalent stress curve of the seal ring end face versus radius is shown in Fig. 7. The equivalent stress of the rotating ring end face is large at the inner diameter and small at the outer diameter,

showing a gradually decreasing trend with the increase of radius. The variation trend of equivalent stress on the stationary ring end face is similar to that of the rotating ring: it decreases rapidly at the initial stage with the increase of radius, slows down when the radius reaches a certain value, and rises slightly at the outer diameter.

4. Influence of Structural Parameters on Deformation of Seal Ring

4.1 Influence of Structural Parameters on Axial Deformation of Seal Ring

In this section, the following main structural parameters are investigated: rotating ring back thickness, stationary ring back thickness, rotating ring back height, stationary ring back height. The single variable method is used to analyze the influence laws of each structural parameter on the deformation and stress of the seal ring.

When the sealing medium pressure is 0.5 MPa, spring specific pressure is 0.15 MPa, and rotating speed is 1500 r/min, it can be seen from Fig. 8, Fig. 9, Fig. 10 and Fig. 11 that, with the increase of the back thickness and back height of the rotating and stationary rings, the maximum axial clearance of Scheme 2 is always smaller than that of Scheme 1. The maximum axial clearances of both seal rings show a gradually decreasing trend.

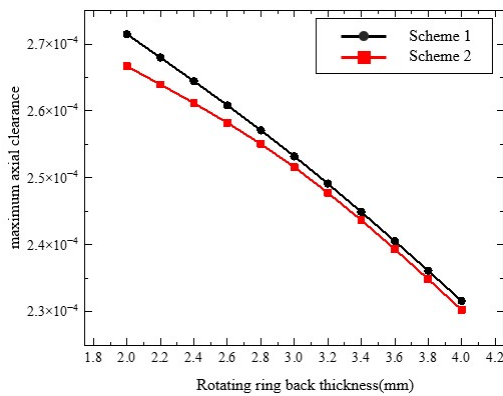


Fig. 8 Influence of Rotating Ring Back Thickness on Axial Clearance of Seal Ring

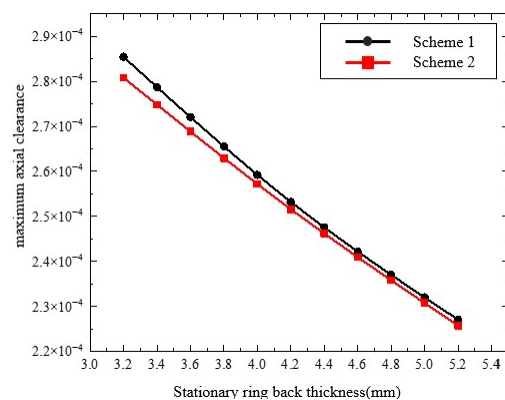


Fig. 9 Influence of Stationary Ring Back Thickness on Axial Clearance of Seal Ring

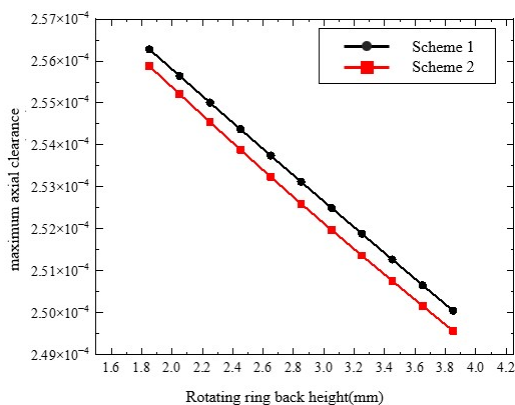


Fig. 10 Influence of Rotating Ring Back Height on Axial Clearance of Seal Ring

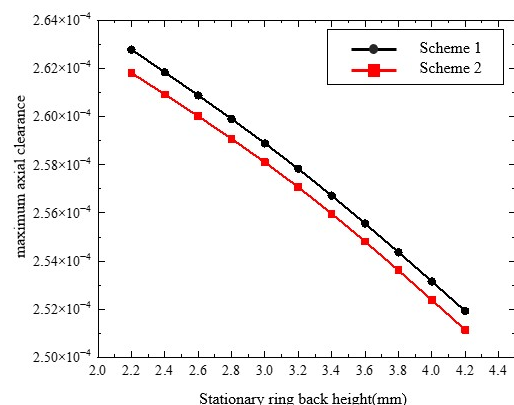


Fig. 11 Influence of Stationary Ring Back Height on Axial Clearance of Seal Ring

4.2 Influence of Structural Parameters on Circumferential Deformation of Seal Ring

It can be seen from Fig. 12, Fig. 13, Fig. 14 and Fig. 15 that the maximum circumferential clearance of the rotating and stationary rings in Scheme 2 is always smaller than that in Scheme 1. With the increase of rotating ring back thickness, the circumferential clearances in both schemes decrease, with a significant drop in the range of 2.0–3.2 mm (obvious stiffness improvement) and a slow decrease

in 3.2–4 mm (stiffness reaches a certain level). As the stationary ring back thickness increases, the clearances in both schemes show a decreasing trend: the rotating ring clearance decreases slowly, while the stationary ring clearance drops sharply in 3.2–4.2 mm and decreases gently in 4.2–5.2 mm. With the increase of rotating ring back height, the rotating ring clearance increases due to larger deformation caused by the increased outer diameter, while the stationary ring clearance decreases because the enlarged heat dissipation area reduces temperature. The stationary ring clearance decreases greatly in 1.85–2.85 mm and slightly in 2.85–3.85 mm. The gap of stationary ring clearance between the two schemes narrows, while that of rotating ring clearance widens. When the stationary ring back height increases, the stationary ring clearance increases due to larger deformation caused by the increased outer diameter, and the rotating ring clearance decreases due to the enlarged heat dissipation area and lower temperature.

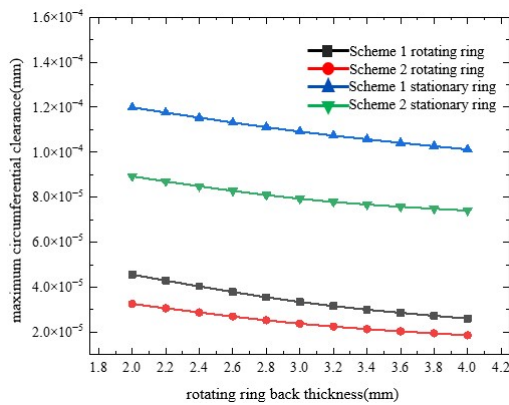


Fig. 12 Influence of Rotating Ring Back Thickness on Circumferential Clearance of Seal Ring

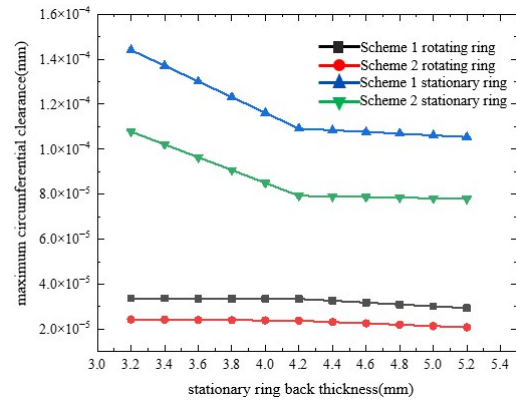


Fig. 13 Influence of Stationary Ring Back Thickness on Circumferential Clearance of Seal Ring

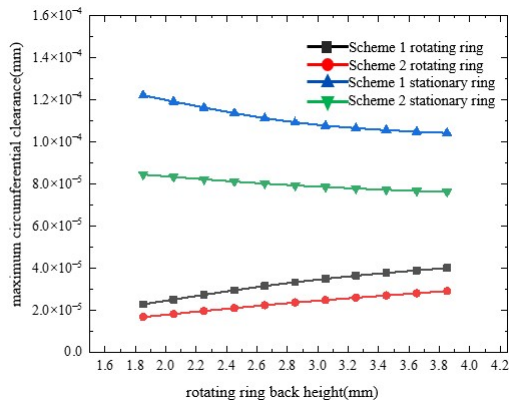


Fig. 14 Influence of Rotating Ring Back Height on Circumferential Clearance of Seal Ring

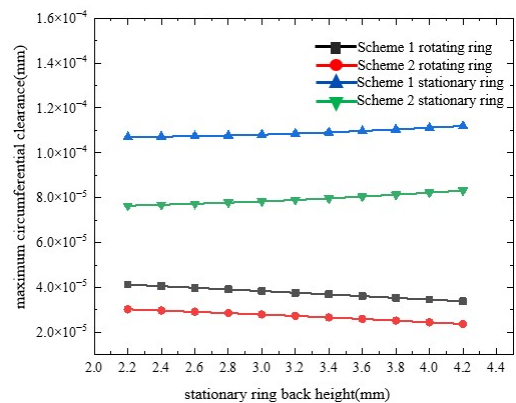


Fig. 15 Influence of Stationary Ring Back Height on Circumferential Clearance of Seal Ring

5. Conclusion

- (1) Based on the conventional split mechanical seal, this paper proposes a novel split mechanical seal structure in which the seal rings and their supporting components are installed with a 90° staggered arrangement.
- (2) Under the thermo-mechanical coupling effect, thermal expansion and deformation occur in the split seal rings. Clearances are formed at both the sealing end face and the split surface of the seal ring, showing a convergent shape from the outside to the inside. The equivalent stress at the sealing

end faces of the rotating and stationary rings gradually decreases with the increase of radius along the radial direction of the seal ring.

(3) The maximum axial and circumferential clearances of Scheme 2 are always smaller than those of Scheme 1. Increasing the back thickness of the rotating and stationary rings increases the section moment of inertia of the seal ring, enhances its bending and torsional stiffness, and improves the deformation resistance. Therefore, the axial clearance and circumferential clearance of the seal ring both show a gradually decreasing trend. With the increase of the rotating ring back height, the axial clearance of the seal ring decreases linearly, the circumferential clearance of the rotating ring increases gradually, and that of the stationary ring decreases gradually. With the increase of the stationary ring back height, the axial clearance of the seal ring decreases gradually, the circumferential clearance of the rotating ring decreases gradually, and that of the stationary ring increases gradually.

References

- [1] Huang Chaolin, Zeng Guanglei, Zhu Quan, et al. Thermo-mechanical Coupling Analysis of Split Mechanical Seal Based on ANSYS[J]. *Mechanical Engineer*, 2024(06): 106-109.
- [2] Song Yupeng. Research on Temperature Rise and Deformation Characteristics of Split Mechanical Seal for Reactors and Experimental Study[D]. Beijing University of Chemical Technology, 2023. DOI: 10.26939/d.cnki.gbhgu.2023.001040.
- [3] Liang Xiao, Zhu Weibing, Wang Fenglin, et al. Failure Analysis and Improvement of Split Mechanical Seal for Reactors Based on FMEA[J]. *Lubrication Engineering*, 2025, 50(02): 170-177.
- [4] Ge Yaping, Shao Aiming, Zhang Liangping, et al. Discussion on Split Mechanical Seal Structure of Marine Stern Shaft[J]. *Times Agricultural Machinery*, 2018, 45(08): 72.
- [5] Hu Qiong, Tao Kai, Sun Jianjun, et al. Numerical Study on Heat Transfer and Coupling Deformation of Split Mechanical Seals[J]. *Lubrication Engineering*, 2018, 43(08): 24-31+86.
- [6] Hu Qiong. Research on Performance of Split Mechanical Seal Based on Multi-field Coupling Effect[D]. Nanjing Forestry University, 2016.
- [7] Wang Gangwei, Wang Juan, Tian Jiabin, et al. Thermo-mechanical Coupling Deformation Characteristics of Submersible Stern Shaft Mechanical Seal[J]. *Ship & Ocean Engineering*, 2022, 51(04): 80-85.
- [8] W Hughes. Phase Change in Liquid Face Seal[J]. *Trans ASME*, 1978, 100(1): 74-79.
- [9] R Slant. Development of an Analytical Model for Use in Mechanical Seal Design[C]. 10th International Conference on Fluid Sealing, BHRA, 1984.
- [10] Chen Huilong, Lin Qinglong, Peng Zhengdong, et al. Thermal-Thermal Stress Coupling Research on Marine Stern Shaft Mechanical Seal [J]. *Ship Engineering*, 2011, 33 (06): 41-44.